Photon spectrum and Absorbed dose in brain tumor

Ángeles Silva-Sanchez[1], Hector Rene Vega-Carrillo[2] and Teodoro Rivera-Montalvo[3]

[1] General Electric Healthcare
Antonio Dovali Jaime 70, Torre A 3er Piso, Col. Santa Fe, 01210, México D.F.

[2] Unidad Académica de Estudios Nucleares de la Universidad Autónoma de Zacatecas
Calle Ciprés 10, Fracc. La Peñuela 98068, Zacatecas, Zacatecas México.

[3] Centro de Investigación en Ciencia y Tecnología Avanzada – IPN
Av. Legaria 694, C.P. 11500, México D.F.

Abstract

Using Monte Carlo methods a BOMAB phantom inside a treatment hall with a brain tumor nearby the pituitary gland was treated with photons produced by a Varian 6 MV linac. The photon spectrum and the absorbed dose were calculated in the tumor, pituitary gland and the head. The treatment beam was collimated to illuminate only the tumor volume; however photons were noticed in the gland. Photon fluence reaching the tumor is 78.1 times larger than the fluence in the pituitary gland, on the other hand the absorbed dose in the tumor is 188 times larger than the dose in the gland because photons that reach the pituitary gland are scattered, by the head and the tumor, through Compton effect.

Keywords: Radiotherapy, Monte Carlo, Phantom, Dose

1. INTRODUCTION

During external-beam radiotherapy inevitably there is radiation that goes away from the treatment field. The out-of-field radiation is composed of photons that scatter from collimators, patient body and radiation that leaks out the accelerator head [Kry *et al*., 2007].

Linear accelerators (LINACs) for radiotherapy working above 8 MV produce undesirable photoneutrons [Hernandez-Adame *et al*., 2001], that have been related to the risk of developing secondary tumors [Newhauser and Durante, 2001; Xu *et al*., 2008]. When photoneutrons are transported in the room induce secondary gamma-rays increasing the dose to the patient, staff and public [Ghassoun *et al*., 2011].

In radiotherapy is essential to minimize the discrepancies between the calculated doses during planning and the doses received by the patient [Verhaegen and Seuntjens 2008]. To verify the applied dose phantoms are used whose geometry and elemental composition is alike to human organs and tissues [ICRU 1989]. Monte Carlo methods have been also used to compare the performance of different treatments without exhibiting the patient [Ge and Faddegon 2011].

Brain tumors have been related to several causes such as: hormonal malfunction [Bolanowski 2011], oncological treatments [Martínez *et al*., 2009], the early exposure to diagnostic x-rays [Pflugbeil *et al*., 2011], fetal of childhood exposure to ultrasound [Rajaraman *et al*., 2011], and to the lead exposure in adults [Bhatti *et al*., 2009].

Tumors deep-seated in the brain are treated trough non-invasive procedures like Boron neutron capture therapy [Barth *et al*., 1992] and radiotherapy with linacs, where a drawback is the dose delivered in tissues around the tumor.

The aim of this work was to determine the photon spectrum and the absorbed dose in tumor, pituitary gland and brain, during radiotherapy treatment with 6 MV photons produced in a linac, where the tumor is adjacent to the pituitary gland.

2. MATERIALS AND METHODS

In order to determine the photon spectra and the dose absorbed the Monte Carlo code MCNP5 [X-5 Monte Carlo team 2003] was used, in the calculations the amount of histories was large enough to have uncertainties less than 1%. In the Monte Carlo calculations are used models that emulate a physical problem the elemental composition of all model components must be as similar as possible to the elemental composition of the real components.

The Bottle Mannequin Absorber phantom (BOMAB) was used to model the patient body, this phantom has legs, arms, pelvis, chest, neck and head. This phantom is filled with different material with dosimetric purposes [Kramer *et al*., 1991; Kramer and Capello 2007]. In the head phantom 1.54 and 0.45 cm-radius spheres were included to model the tumor and the pituitary gland respectively. The elemental concentration used to model the tumor was the same as the carcinoma [Maughan *et al*., 1999], the phantom elemental composition was tissue equivalent [ICRU 1989]. In table 1 are shown the elemental composition of the human brain, tissue equivalent and carcinoma.

Table 1.- Elemental composition used to modeling the human brain, tissue equivalent and carcinoma.

Organ	Composition [o/w]					Density
	H	C	N	O	Others	[g cm^{-3}]
Brain	10.7	14.5	2.2	71.2	0.2 Na, 0.4 P, 0.2 S, 0.3 Cl, 0.3 K	1.04
Tissue equivalent	10.1	11.1	2.6	76.2	-	1.04
Carcinoma	10	18.5	4.2	65.9	1.4 others	1.50

The pituitary gland was located adjacent to the tumor, as is shown in figure 1, to avoid the irradiation of the gland the beam was addressed laterally in two directions along x-axis.

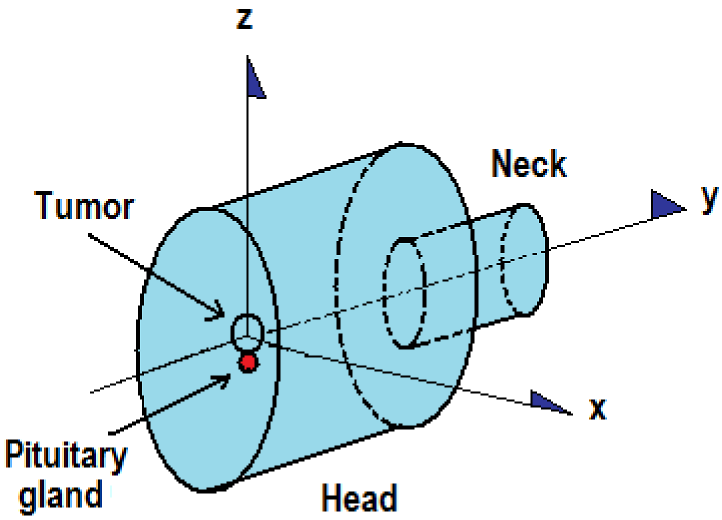

Figure 1.- BOMAB phantom´s head with the pituitary gland and the tumor.

The accelerator head was modeled as a 15 cm-thick tungsten spherical shell, at its center a point-like source was located, the energy distribution of the source term, shown in figure 2, was the photon spectrum of a Varian 6 MV linac [Sheikh-Bagheri and Rogers 2002].

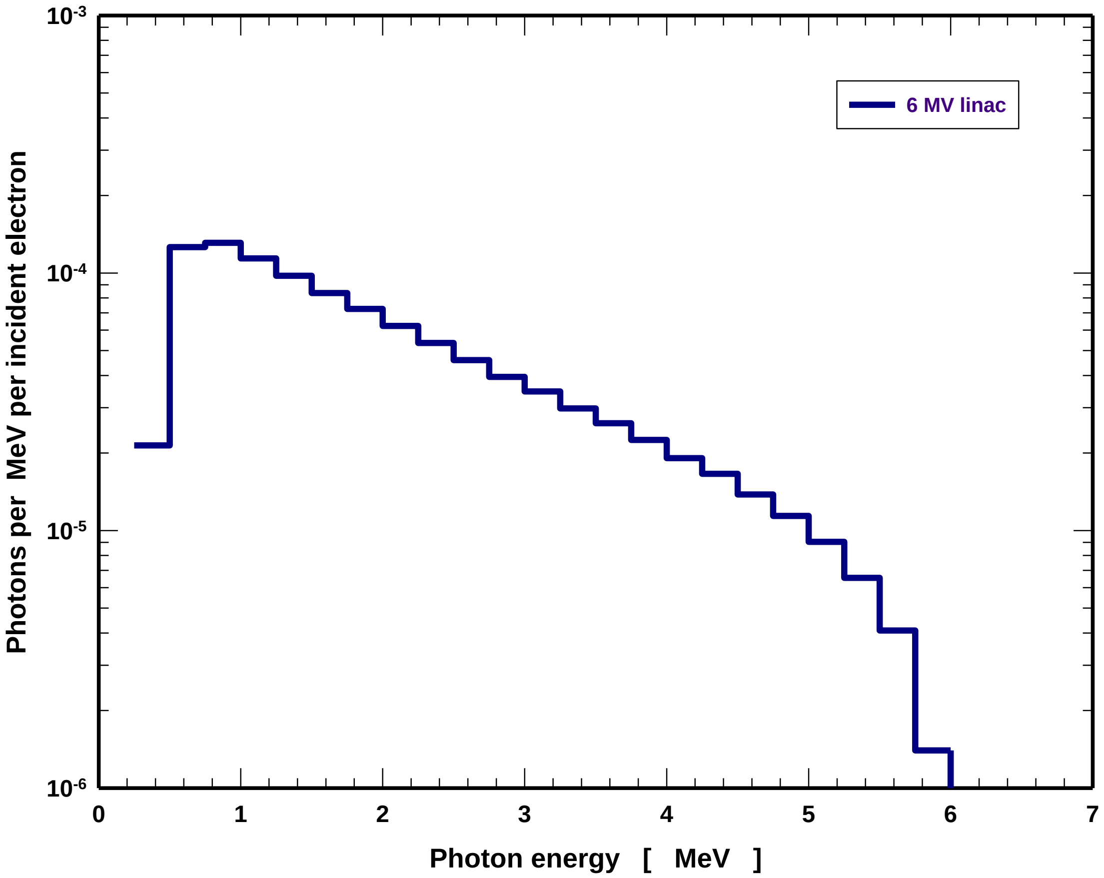

Figure 2.- Photon spectrum of the 6 MV Varian linac.

The linac head and the BOMAB were located in a concrete spherical shell with air, modeling the treatment room, as is shown in figure 3.

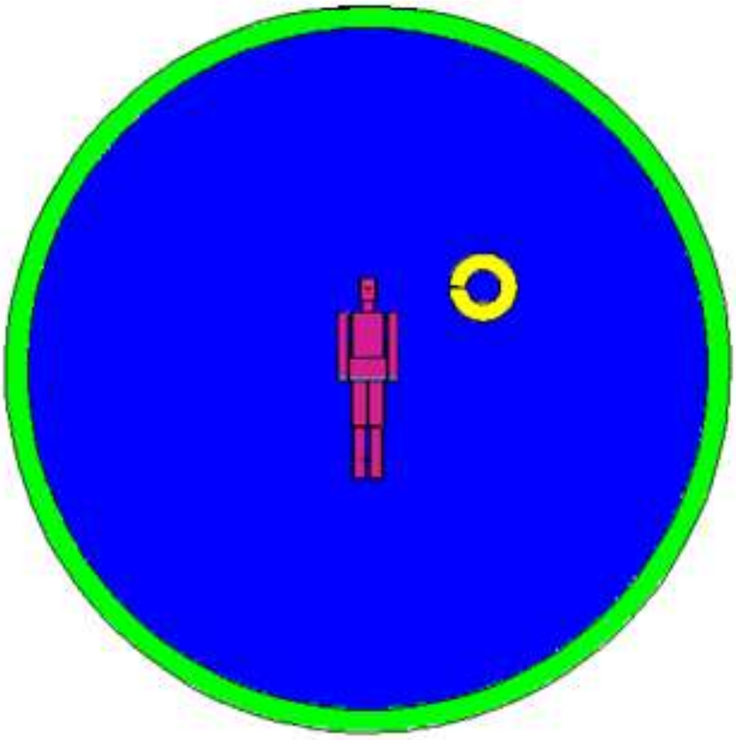

Figure 3.- Monte Carlo model.

In the linac-head model a small aperture was included to irradiate only the tumor volume. The distance between the center of the tumor and the center of the linac-head was 100 cm. With this model the photon spectrum and the absorbed dose in the tumor, the pituitary gland and the BOMAB head were estimated.

3.- RESULTS

Photon spectrum and absorbed dose in the pituitary gland, tumor and BOMAB head, when the therapeutic beam was sent form the left was similar when the beam was addressed from the right. The photon spectrum in the pituitary, tumor and BOMAB head when the beam was sent from the right is shown in figure 4.

In table 2 are shown the absorbed doses, in Gy per photon emitted by the linac´s head, in the pituitary gland, the tumor and the BOMAB head.

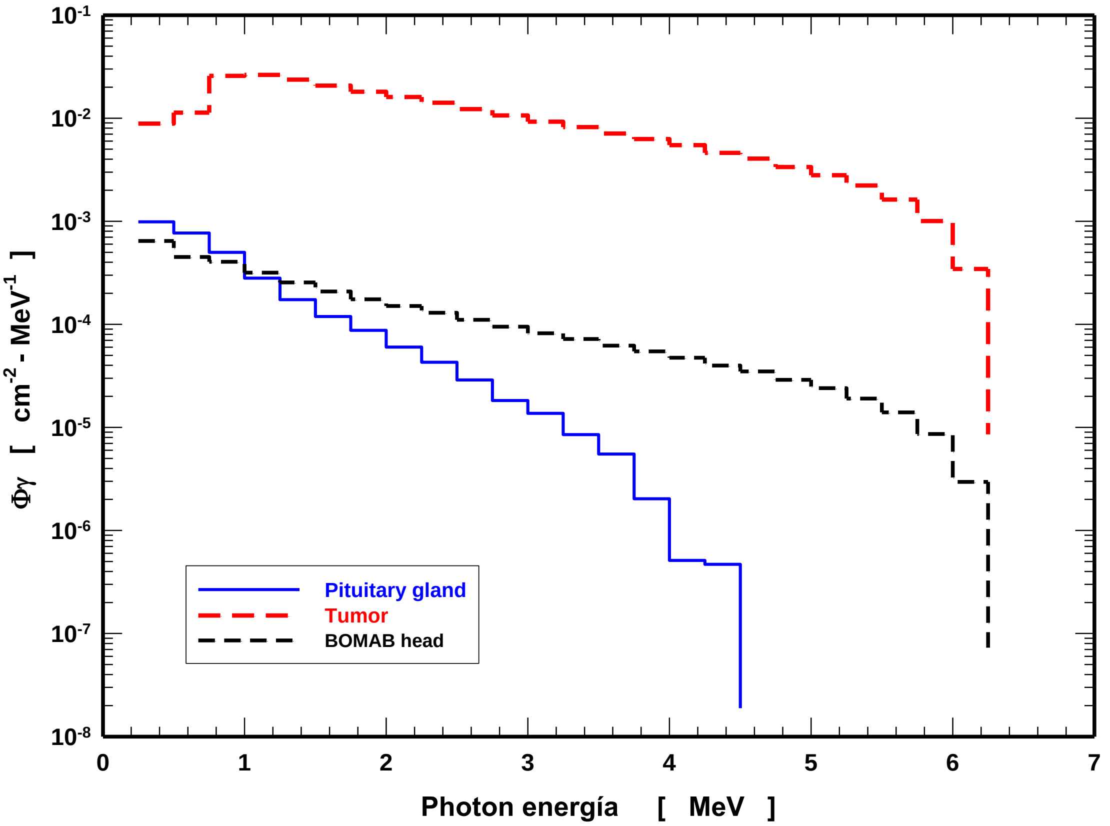

Figure 4.- Photon spectra.

Table 2. Absorbed doses in the pituitary gland, tumor and the head phantom.

Site	Absorbed dose [Gy]
Pituitary gland	1.4259E(-16) ± 0.06%
Tumor	2.6777E(-14) ± 0.01%
BOMAB Head	2.7607E(-16) ± 0.01%

4.- DISCUSSION

Photon spectrum in the tumor has approximately the same shape as the spectrum produced by the source term. The difference is explained as follows: as source-term photons are transported into the brain some are scattered through Compton interactions and lower energy photons emerge; also, pair production are induced and when positron annihilation occur 0.511 MeV photons are produced enhancing the amount of low energy photons.

Nevertheless the treatment beam was collimated to shape the tumor; photons are noticed in the pituitary gland. The total photon fluence in the tumor is 73.9 and 70.6 times larger than photon fluence in the pituitary gland and the BOMAB head respectively. Thus, photon fluence in the head in approximately 4.8% larger that the fluence in the pituitary gland. The photon spectrum in the head has energies from 0.25 up to 6 MeV, being alike the source-term spectrum, while the photon spectrum in the pituitary gland has energies from 0.25 up to 4.25 MeV these photons are mainly scattered from the tumor and secondly by the brain tissue. Scattered photons have less energy than those reaching the tumor.

The importance of changes in the photon spectrum can be noticed in the absorbed dose that is larger in the tumor being 187.8 and 96.9 times larger than absorbed doses in the gland and the head respectively. Thus, the dose in the head is 93.6% larger that the dose in the gland.

4.- CONCLUSIONS

Using Monte Carlo methods the photon spectra and the absorbed dose has been estimated in a tumor located near to the pituitary gland when is treated with photons produced by a Varian 6 MV linac. In the calculations a full BOMAB phantom was used comparing the spectra and doses in the pituitary gland and the phantom head.

Nevertheless the incoming beam was conformed to the tumor; scattered photons reach the pituitary gland, with lower energy than the incoming photons.

The absorbed dose in the tumor is approximately 187.8 times larger than the fluence in the pituitary gland.

Acknowledgments

The first author, ASS, wants to thanks to CONACyT (Mexico) by the scholarship.

REFERENCES

Barth RF; Soloway AH; Fairchild RG; Brugger RM. (1992). *Boron neutron capture therapy for cancer. Realities and prospects*. Cancer **70**: 2995-3007.

Bolanowski M. (2011). *Pituitary late effects of radiotherapy for brain tumours*. Endocrine Abstracts **26**: S17.3.

Bhatti P; Stewart PA; Hutchinson A; Rothman N; Linet MS; Inskip PD; Rajarman P. (2009). *Lead exposure, polymorphisms in genes related to oxidative stress, and risk of adult brain tumors*. Cancer Epidemiology Biomarkers & Prevention **18**: 1841-1848.

Ge Y; Faddegon BA. (2011). *Study of intensity-modulated photon-electron radiation therapy using digital phantoms*. Physics in Medicine and Biology **56**: 6693-6708.

Ghassoun J; Senhou N; Jehouani A. (2011). *Neutron and photon doses in high energy radiotherapy facilities and evaluation of shielding performance by Monte Carlo method*. Annals of Nuclear Energy **38**: 2163-2167.

Hernandez-Adame L; Contreras-Sandoval H; Vega-Carrillo HR; Perez-Landeros LH. (2011). *Design of a treatment room for an 18-MV linac*. Nuclear Technology **175**: 105-112.

ICRU. (1989). *Tissue substitutes in radiation dosimetry and measurement*. ICRU Report 44. International Commission on Radiation Units and Measurements. Bethesda MD.

Kramer GH; Burns L; Noel L. (1991). *The BRMD BOMAB phantom family*. Health Physics **61**: 895-902.

Kramer GH; Capello K. (2007). *The standfast whole body counter: Efficiency as a function of BOMAB phantom size and energy modeled by MCNP5*. Health Physics **92**: 290-296.

Maughan RL; Chuba P; Porter AT; Ben-Josef E; Lucas DR; Bjarngard E. (1999). *Mass energy-absorption coefficients and mass collision stopping powers for electrons in tumors of various histologies*. Medical Physics **26**: 472-477.

Martínez A; Suárez M; Jasper H; Pasqualini T; Rey R; Gottlieb S. (2009). *Secuelas endocrinológicas del tratamiento de las enfermedades oncológicas en la infancia y la adolecencia*. Revista Argentina de Endocrinologia y Metabolismo **46**: 24-38.

Pflugbeil S; Pflugbeil C; Schmitz-Feuerhake I. (2011). *Risk estimates for meningiomas and other late effects after diagnostic x-ray exposure of the skull*. Radiation Protection and Dosimetry **147**: 305-309.

Rajaraman P; Simpson J; Neta G; Berrington de Gonzalez A; Ansell P; Linet MS; Ron MS; Roman E. (2011). *Early life exposure to diagnostic radiation and ultrasound scans and risk of childhood cancer: Case-control study*. British Medical Journal **342**: 1-9.

Sheikh-Bagheri D; Rogers DWO. (2002). *Monte Carlo calculation of nine megavoltage photon beam spectra using the BEAM code*. Medical Physics **29**: 391-402.

Verhaegen F; Seuntjens J. (2008). *Monte Carlo modeling of external radiotherapy photon beams*. Physics in Medicine and Biology **48**: R107-R164.

Xu XG; Bednarz B; Paganetti H. (2008). *A review of dosimetry studies on external-beam radiation treatment with respect to second cancer induction*. Physics in Medicine and Biology **53**: R193-R41.

X-5 Monte Carlo team. (2003). *MCNP – a general Monte Carlo N-particle transport code, version 5*. **Report LA-UR-03-1987** Los Alamos National Laboratory. USA.